Lab on a Chip

Cite this: *Lab Chip*, 2012, **12**, 1753

www.rsc.org/loc

CRITICAL REVIEW

# Microfluidic approaches for cancer cell detection, characterization, and separation

**Jian Chen,[a] Jason Li[bc] and Yu Sun*[bcd]**

***Received 21st December 2011, Accepted 10th February 2012***
**DOI: 10.1039/c2lc21273k**



This article reviews the recent developments in microfluidic technologies for *in vitro* cancer diagnosis. We summarize the working principles and experimental results of key microfluidic platforms for cancer cell detection, characterization, and separation based on cell-affinity micro-chromatography, magnetic activated micro-sorting, and cellular biophysics (*e.g.*, cell size and mechanical and electrical properties). We examine the advantages and limitations of each technique and discuss future research opportunities for improving device throughput and purity, and for enabling on-chip analysis of captured cancer cells.

## 1 Introduction

Cancer is a class of diseases characterized by the uncontrolled growth of cells that ultimately invade surrounding tissues and metastasize to distant sites within the body.[1,2] Early cancer detection is crucial for improved prognosis and cancer management due to the small tumor size and localization of the tumor at the primary site.[3–6] Conventional cancer cell sorting techniques, which have been reviewed elsewhere,[7–11] including centrifugation, chromatography, and fluorescence and magnetic-activated cell sorting, are limited in yield and purity and further rely on the expertise and subjective judgments of highly skilled personnel.

The small sample volumes, fast processing times, multiplexing capabilities, and large surface-to-volume ratios inherent in microfluidic systems[12,13] offer new opportunities for cytology and cytopathology,[14–25] particularly for *in vitro* cell sorting and detection.[17,26–32] Leveraging these advantages, various microfluidic platforms have been developed for capturing rare cells including circulating tumor cells (CTCs), circulating fetal cells, and stem cells. Microfluidic sorting of rare cells has been reviewed elsewhere.[31,33–35] In this review, we focus on the application of microfluidic systems for cancer cell detection and sorting. We first present the development and working principle of several key microfluidic platforms including those based on cell-affinity chromatography,[36–53] magnetic activated cell sorting,[54–63] and differences in cellular biophysics (*e.g.*, cell size,[64–77] adhesion,[42,78,79] deformability,[80–86] dielectrophoresis (DEP),[76,87–117] and impedance[85,118–121]). We discuss the performance and capabilities of each system in terms of throughput, yield, purity, cell viability, and the capability for on-chip post-processing after cancer cell capture.

## 2 Cell-affinity micro-chromatography

Cell-affinity chromatography[31] is a method that selectively captures suspended cancer cells from a heterogeneous cell population through selective binding with substrate-immobilized high-affinity ligands, thereby separating cancer and healthy cells (see summary in Table 1). Du and Gollahon *et al.* reported the first antibody-based cell-affinity micro-chromatography system for capturing cervical cancer cell lines by binding α6-integrins, which served as capture ligands, onto the surfaces of a polydimethylsiloxane (PDMS) microchannel.[36] Device characterization with cell line mixtures of normal human glandular epithelial, human cervical stromal and cervical cancer cells with up-regulated α6-integrin cell surface receptors demonstrated a cancer cell recovery rate greater than 30%, while 5% of the captured cells were normal cells. Du and Gollahon *et al.* further adapted the technique for capturing breast cancer cells[38] and additionally proposed a cell detachment model that highlights the importance of three device parameters (sample flow rate, antibody selection, and channel geometry) for achieving high cell capture and identification yield.[37]

By flowing cells through a dense array of functionalized silicon micro-pillars to enhance the likelihood of cell–antibody interactions as compared to a simple microfluidic channel, Nagrath and Toner *et al.* demonstrated the ability to separate CTCs from patient whole blood using microfluidic cell-affinity chromatography (CTC chip; Fig. 1(a)).[39,41] The CTC chip contained 78 000 freestanding micro-pillars (100 μm tall, 100 μm in diameter) functionalized with anti-epithelial-adhesion-molecule antibodies (Anti-EpCAM), representing a total surface area of 970 $mm^2$. With optimized flow velocity and shear force around the micro-posts, the CTC chip was capable of processing millilitres

[a]*State Key Laboratory of Transducer Technology, Institute of Electronics, Chinese Academy of Sciences, Beijing, 100190, P.R. China*
[b]*Institute of Biomaterials and Biomedical Engineering, University of Toronto, Toronto, ON, M5S 3G8, Canada. E-mail: sun@mie.utoronto.ca; Fax: +1 416-978-7753; Tel: +1 416-946-0549*
[c]*Department of Mechanical and Industrial Engineering, University of Toronto, Toronto, ON, M5S 3G8, Canada*
[d]*Department of Electrical and Computer Engineering, University of Toronto, Toronto, ON, M5S 3G4, Canada*

**Table 1** Microfluidic devices based on cell-affinity micro-chromatography for cancer cell capture

| Cell capture structures | Targeted cells | Carrier medium and control cells | Target cell recovery rate | Capture purity |
|---|---|---|---|---|
| α6-integrin + PDMS flat micro-channels[36] | Human cervical cancer cells | Human glandular epithelial cells and cervical stromal cells + PBS | >30% (targeted cancer cell capture) | <5% (capture of normal cells) |
| Epithelial membrane antigen and epithelial growth factor receptor + PDMS flat micro-channels[38] | Human breast cancer cells of TTU-1 | Human mammary epithelial cells + PBS | >30% (targeted cancer cell capture) | <5% (capture of normal cells) |
| Anti-epithelial-cell-adhesion-molecule (EpCAM) antibodies + silicon micro-posts[39] | Human non-small-cell lung cancer cells of NCI-H1650, breast cancer cells of SK-Br-3, prostate cancer cells of PC3-9 and bladder cancer cells of T-24 | PBS (100 cancer cells per ml) or blood samples from healthy donors (50–50 000 NCI-H1650 cells per ml) | >65% in PBS and >60% in whole blood samples | NA |
| Anti-EpCAM + silicon micro-posts[39] | CTCs | Blood samples from patients with non-small-cell lung cancer, prostate, pancreatic, breast and colon cancer | CTC identification in 115 of 116 patient samples with metastatic cancer and in 7/7 patients with early-stage prostate cancer | ~50% |
| Anti-EpCAM + silicon micro-posts[41] | CTCs | Blood samples from patients with non-small-cell lung cancer | CTC identification in all patients ($n = 27$) | NA |
| Anti-EpCAM + PDMS micro-channels with patterned herringbones[45] | Human prostate cancer cells of PC3 | Blood samples from healthy donors (1000 PC3 cells per ml) | 91.8% ± 5.2% | NA |
| Anti-EpCAM + PDMS micro-channels with patterned herringbones[45] | CTCs | Blood samples from patients with metastatic prostate cancer | CTC identification in 14 of 15 patient samples (93%) | NA |
| Antibody (J591) targeting prostate-specific membrane antigen (PSMA) + optimized silicon micro-posts[44] | Human prostate cancer cells expressing PSMA | PBS or blood samples from healthy donors (150–220 cells per ml) | 97% ± 3% in PBS and 85% ± 5% in whole blood samples | 68% ± 6% in whole blood samples |
| Antibody (J591) targeting prostate-specific membrane antigen (PSMA) + optimized silicon micro-posts[44] | CTCs | Blood samples from patients with prostate cancer | CTC identification in 18 of 20 patient samples (90%) | 62% ± 2% |
| Anti-EpCAM + 3D nanostructured silicon substrates[43] | Human breast cancer cells of MCF-7 | Culture medium ($10^5$ cells per ml) or rabbit blood samples (5–1250 cells per ml) | 45–65% in culture medium and >40% in blood samples | NA |
| Anti-EpCAM + 3D silicon nanostructured substrates + overlaid PDMS serpentine channels[49] | Human breast cancer cells of MCF-7, prostate cancer cells of PC3 and bladder cancer cells of T24 | Culture medium (100 MCF-7, PC3 or T24 cells per ml) or rabbit blood samples (50–1000 MCF-7 cells per ml) | >95% in both culture medium and rabbit blood samples | NA |
| Anti-EpCAM + 3D silicon nanostructured substrates + overlaid PDMS serpentine channels[49] | CTCs | Blood samples from patients with prostate cancer | CTC identification in 17 out of 26 patient blood samples | NA |
| DNA-aptamer + PDMS flat micro-channels[52] | Human leukemic cells of CCRF-CEM | Human leukemic cells of NB-4 + PBS | >80% | >97% |
| DNA-aptamer + PDMS flat micro-channels[53] | Human leukemic cells of CCRF-CEM, Ramos and Toledo | PBS | 83% ± 9% of CCRF-CEM, 61% ± 14% of Ramos and 50% ± 10% of Toledo | 97% of CCRF-CEM, 97% of Ramos and 88% of Toledo |
| Anti-EpCAM + high-aspect ratio PMMA micro-channels with sinusoidal configurations[40] | Human breast cancer cells of MCF-7 | Rabbit blood (10 cells per ml) | >97% | NA |
| DNA-aptamers + high-aspect ratio PMMA curvilinear micro-channels[51] | Human prostate cancer cells of LNCaP | Rabbit blood (20 cells per ml) | 90% | 100% |
| Anti-EpCAM + high-aspect ratio PMMA micro-channels with sinusoidal configurations[47] | Human colorectal cancer cells of SW620 and HT29 | Rabbit blood (10 SW620 cells or 32 HT29 cells per ml) | 96% ± 4% | NA |

**Table 1** (*Contd.*)

| Cell capture structures | Targeted cells | Carrier medium and control cells | Target cell recovery rate | Capture purity |
|---|---|---|---|---|
| N-cadherin antibodies + flat PDMS–silicon hybrid micro-channels[42] | Human breast cancer cells of MDA-231-N and prostate cancer cells of PC3N | Human breast cancer cells of MDA-231 (cadherin-11) as well as BT20 (E-cadherin) + PBS | >90% ± 3% (MDA-MB-231-N and PC3N) | <10% ± 3% (MDA-MB-231 and BT20) |
| Cadherin-11 antibodies + flat PDMS–silicon hybrid micro-channels[50] | Human breast cancer cells of MDA-231 (cadherin-11) | Human breast cancer cells of BT20 (E-cadherin) + PBS | >95% | 85%–95% (MDA-MB-231 : BT20 = 1 : 1000) |
| Herceptin + PDMS micro-posts[46] | Human breast cancer cells of SK-Br-3 | Blood samples from healthy donors ($2 \times 10^3$ to $2 \times 10^4$ SK-Br-3 cells per ml) | ~80% | NA |
| Anti-EpCAM + PDMS micro-posts[48] | Human small-cell lung cancer cells of H69 and breast cancer cells of SK-Br-3 | PBS or whole blood samples from healthy donors ($2 \times 10^3$ to $2 \times 10^4$ SK-Br-3 cells per ml) | 80%–90% in PBS and >70% in whole blood samples | NA |



of whole blood within a short time frame and successfully identified CTCs in 115 out of 116 samples derived from cancer patients (metastatic lung, prostate, pancreatic, breast and colon cancer) with approximately 50% purity. Application of the CTC chip in clinical trials successfully isolated CTCs in 7/7 patients with early-stage prostate cancer, further demonstrating the promise of this technology.

The "herringbone chip" (see Fig. 1(b)), a second generation CTC chip developed by Stott and Toner *et al.*, introduced a different microchannel architecture that produced micro-vortices within the flow to further improve the likelihood of cell–surface interactions and achieved a high cell recovery rate (91.8% ± 5.2% for prostate cancer cells). This technique was also effective in detecting CTCs in 14 out of 15 patients with metastatic prostate cancer.[45] Using a similar design, Gleghorn and Kirby *et al.* developed a geometrically optimized micro-post-array designed to maximize streamline distortion to enhance the interaction between cancer cells and the micro-posts, resulting in a 90% CTC recovery rate for human samples ($n = 20$) and a higher sample purity of 62% ± 2%.[44]

An alternative strategy for improving cell–surface interaction is the use of a 3D nano-structured substrate surface in lieu of smooth micron-sized posts and surfaces. Coating of the nano-structured surface with anti-EpCAM resulted in a higher cancer cell recovery rate due to topographic interactions between the silicon nano-pillar substrate and the nanoscale components found on the cell surface.[43] Microfluidic channels with densely packed silicon nano-pillar surfaces (100–200 nm in diameter) enabled the capture of up to ten times more cells as compared to channels with flat substrates. Integration of this nano-structured surface with a serpentine chaotic mixing PDMS channel (see Fig. 1(c)) resulted in a device with a cell recovery rate greater than 95% for MCF-7 cells spiked into whole blood. Compared to the conventional CellSearch assay, a significantly higher number of CTCs were captured in 17 out of 26 blood samples from patients with prostate cancer.[49]

Due to the limited availability of highly selective antibodies for capturing targeted cancer cells, aptamers have recently been employed as binding ligands in microfluidic devices for cancer cell detection.[51–53] Compared to antibodies, aptamers can be created without knowledge of the explicit molecular signature that differentiates cancer cells from healthy cells.[122] Phillips and Tan *et al.* reported the first microfluidic use of aptamers for cancer cell enrichment by immobilizing aptamers onto the surface of flat microchannels. This system achieved a recovery rate higher than 80% and purity better than 97%.[52] Using a second-generation device, Phillips and Tan further demonstrated cell-type dependent enrichment, where three types of cancer cells were captured by independent capture domains with high recovery rates and purity.[53]

In addition to selective cancer cell capture, cell-affinity micro-chromatography techniques may be integrated with other microfluidic components to enable subsequent on-chip analysis including enumeration, manipulation, and molecular identification.[40,47,51] For example, SW620 and HT29 cells (colorectal cancer cell lines) mixed into whole blood samples were used as a model to demonstrate on-chip selection, enumeration and collection.[47] Selected CTCs were enzymatically released from the antibody surface and hydrodynamically transported through a pair of Pt electrodes for conductivity-based enumeration. Following enumeration, the CTCs were electrophoretically withdrawn from the bulk hydrodynamic flow for point mutation analysis using PCR/LDR/capillary electrophoresis assays.

## 3 Magnetic activated micro-cell sorters

Magnetic activated cell sorting relies on the interaction between cell surface antigens and antibodies conjugated to suspended magnetic particles.[35] Compared to cell-affinity micro-chromatography, where the retrieval of captured cancer cells can be difficult, magnetic bead-based techniques readily permit the manipulation of captured cancer cells using local magnetic fields (see summary in Table 2). Liu and Pang *et al.* demonstrated the first microfluidic device for isolating low-abundance cancer cells from a red blood cell (RBC) suspension using magnetic cell separation (see Fig. 2(a)).[55] In this system, a hexagonal array of nickel micro-pillars was integrated onto the bottom of a microfluidic channel and used to generate magnetic field gradients to efficiently trap superparamagnetic beads. The trapped magnetic beads functioned as a capture zone, followed by *in situ* chemical and biological modifications to functionalize the surface of beads with specific antibodies. Based on the interaction between the

specific antibodies and *N*-acetylglucosamine on the cell membrane, A549 cancer cells spiked in RBCs were effectively captured and sorted on the microfluidic device with a capture rate between 62% and 74%.

Antibody-coated magnetic beads were also used in a microfluidic device for the serial selection of cell subpopulations.[57] As illustrated in Fig. 2(b), this separation system consists of two separate compartments, each containing magnetic beads functionalized with different surface membrane protein receptors specific to prostate cancer cells (PSMA and CD10). As a cell suspension is introduced to the first array, the cells expressing CD10 are immobilized onto the magnetic beads while CD10− cells pass through this chamber and into the second compartment. PSMA+ cells bind to the magnetic beads located in the second compartment after which the remaining cells are flushed from the system. Thus, PSMA+/CD10− and CD10+ prostate cancer cell subpopulations can be isolated.

In order to further increase the surface-to-volume ratio of magnetic beads for cell sorting, Saliba and Viovy *et al.* developed a method using columns of bio-functionalized super-paramagnetic beads self-assembled in a microfluidic channel.[60] In this system, a hexagonal array of magnetic ink was first patterned at the bottom of microfluidic channels. Beads coated with antibodies were then injected into the channel and allowed to settle down. Upon application of an external vertical magnetic field, the magentic beads assembled on top of the ink dots to form a regular array of columns. Tests using cell line mixtures demonstrated a capture recovery rate greater than 94% and the capability to cultivate the captured cells on chip. Furthermore, clinical samples (blood, pleural effusion, and fine needle aspirates) from healthy donors and patients with B-cell hematological malignant tumors were analyzed in the microfluidic chamber.

Multi-functional, integrated microfluidic devices capable of cancer cell separation, cell lysis and genetic identification were reported by Lien and Lee.[59] This platform consisted of an incubation module where target cancer cells are selectively captured onto functionalized magnetic beads, a control module for sample transportation, and a nucleic acid amplification module for cell lysis and genetic identification (see Fig. 2(c)). Cancer cells (*e.g.*, lung and ovarian carcinoma) were spiked into whole blood samples and loaded into the incubation chamber with pre-loaded magnetic beads coated with monoclonal antibodies. The cancer cells were specifically immobilized onto the surface of the magnetic beads with a recovery rate higher than 90%. The purified magnetic complexes were subsequently re-suspended and transported to the cell lysis/reverse transcription chamber where the expressed genes associated with ovarian and lung cancer cells were successfully amplified.

## 4 Size-based cancer cell capture and separation

Differences in cell size can be exploited for microfluidic cancer cell selection without the knowledge of target cells' biochemical characteristics.[32] Size-based cell separation is attractive, for instance, for capturing CTCs since these cells are much larger

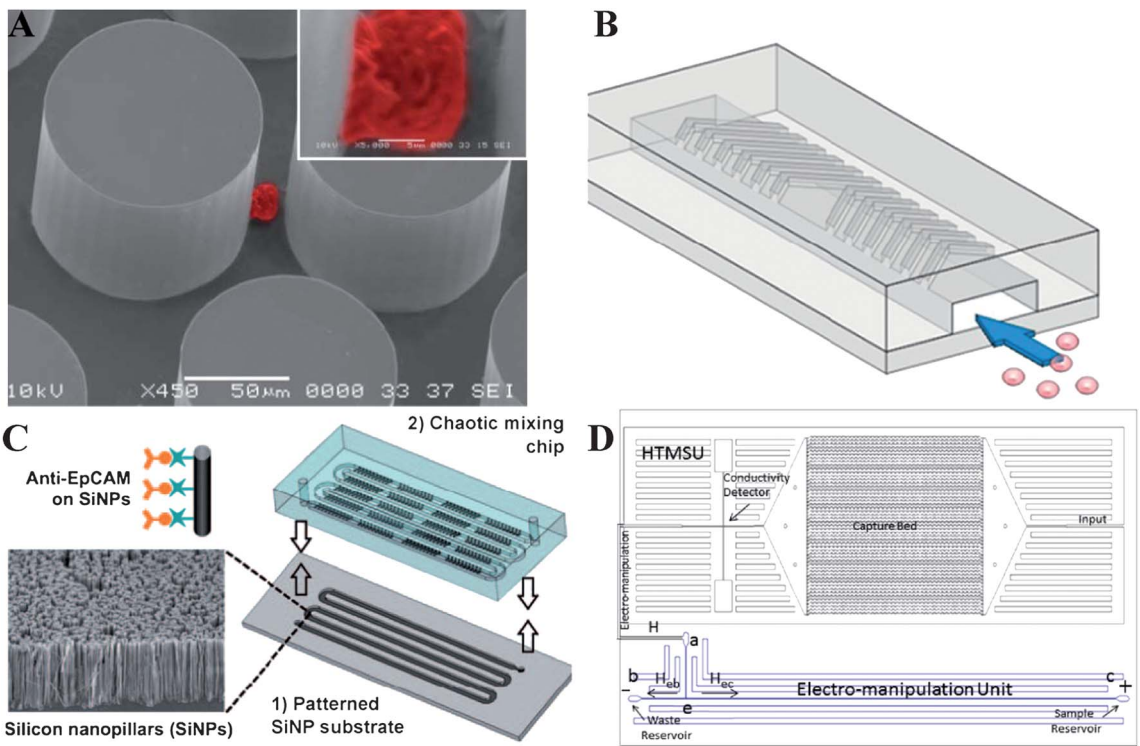


**Fig. 1** Cell-affinity micro-chromatography for cancer cell capture. (a) Micro-pillars on CTC-chip captured a NCI-H1650 lung cancer cell spiked into blood. Reproduced with permission from ref. 39. (b) Herringbone grooves for enhancing CTC isolation due to passive mixing. Reproduced with permission from ref. 45. (c) A CTC isolation micro-device using a 3D nano-structured substrate integrated with an overlaid serpentine chaotic mixing channel. Reproduced with permission from ref. 49. (d) An integrated microfluidic device for cancer cell capture and post-capture processing including the release of captured cancer cells, on-chip enumeration and electro-manipulation. Reproduced with permission from ref. 47.

 

**Table 2** Magnetic activated micro-cell sorters for cancer cell capture

| Cell capture structures | Targeted cells | Carrier medium and control cells | Target cell recovery rate | Capture purity |
|---|---|---|---|---|
| A nickel micropillar array + magnetic beads functionalized with wheat germ agglutinin[55] | Human lung cancer cells of A549 | Human RBCs + culture medium | 62%–74% | ~93% (initial ratio A549 : RBCs = 1 : 10) |
| A paramagnetic array of 80% Ni and 20% Fe + magnetic beads complementary to anti-CD10 antibodies in chamber 1 and anti-PSMA antibodies in chamber 2[57] | Human prostate cancer cells of LNCaP incubated with PSMA antibodies | LNCaP incubated with CD10 antibodies + PBS | 50%–70% of LNCaP incubated with PSMA antibodies in chamber 2 | ~10% of LNCaP incubated with CD10 antibodies in chamber 2 (initial mixture ratio of 1 : 1) |
| External permanent magnet + magnetic beads coated with Anti-EpCAM (Ber-EP4)[59] | Human ovarian cancer cells of BG-1 and lung cancer cells of AS2 | Blood samples from healthy donors ($10^6$ cells per ml) | ~95.1% for BG-1 cells and 92.7% for AS2 cells | NA |
| An array of magnetic dots + self-assembled magnetic beads coated with anti-CD19 antibodies[60] | Human lymphoma cells of Raji CCL-86 | Human lymphoma cells of Jurkat TIB152 + PBS ($2 \times 10^6$ cells per ml) | 97% ± 2% of Raji cells | <2% (capture of Jurkat TIB152 cells) |
| An array of magnetic dots + self-assembled magnetic beads coated with anti-CD19 antibodies[60] | B-cell hematological malignant tumors (leukemia and lymphoma) | Clinical samples (blood, pleural effusion, and fine needle aspirates) from chronic lymphocytic leukemia, mantle cell lymphoma, follicular lymphoma and two healthy volunteers | Consistent immunophenotype and morphology results with those obtained by flow cytometry | |
| External permanent magnet + self-assembled magnetic bead patterns coated with 5D10 antibodies[61] | Human breast cancer cells of MCF-7 | Human lymphoma cells of Jurkat TIB152 + PBS ($10^6$ cells per ml for both MCF-7 and Jurkat cells) | 85% ± 10% of MCF-7 cells | <5% (capture of Jurkat TIB152 cells) |
| A nickel micropillar array + magnetic beads functionalized with wheat germ agglutinin[62] | Human lung cancer cells of A549 | PBS | A total mass of 90.6 ng of captured A549 cells | |
| External permanent magnet + $Fe_3O_4$ magnetic nanoparticles conjugated to Anti-EpCAM[137] | Human colon cancer cells of COLO205 and human breast cancer cells of SK-BR-3 | Blood samples from healthy donors | 90% and 86% for COLO205 and SK-BR-3 cells, respectively | NA |



than other cells found in whole blood (see summary in Table 3). Mohamed *et al.* reported the first size-based microfluidic cancer cell separation device which featured on-chip micro-filters.[64] The device consisted of four regions with decreasing channel widths (20 μm, 15 μm, 10 μm, and 5 μm) and a constant channel depth (20 μm). Cultured neuroblastoma cells mixed with whole blood were injected into the device where the 10 μm wide channels trapped the cancer cells.

Size-exclusive membrane filters were also proposed for cancer cell detection and separation. Zheng and Tai *et al.* developed a parylene membrane micro-filter device with circular holes (10 μm diameter) with a center to center distance between adjacent pores of 20 μm.[66] The size difference between CTCs and human blood cells was exploited to test 57 blood samples from patients with metastatic prostate, breast, colon, or bladder cancer. The results demonstrated CTC capture and identification in 51 of 57 patients compared with only 26 patients in 57 patients using the conventional CellSearch method.[72] However, this process resulted in low capture cell viability due to the large stresses that developed in the cell membrane during the cell capture process. Zheng and Tai *et al.* further developed a double-membrane device to decrease stresses experienced by the cell membrane during the trapping process, and the device enabled *via* CTC capture (see Fig. 3(a)).[77] In this device, a second porous membrane was incorporated below the first membrane. The pore positions between the two membranes were intentionally misaligned. This bottom membrane provided support for the trapped cells to effectively reduce flow-induced stress on the cell membrane.

In order to facilitate the retrieval of captured cancer cells, Tan and Lim *et al.* developed a microfluidic device with multiple arrays of crescent-shaped wells (see Fig. 3(b)) to isolate cancer cells from spiked blood[68] and patient whole-blood samples.[73] Gaps (5 μm) were made within each of the crescent-shaped traps to ensure the complete removal of other blood constituents due to their ability to traverse narrow constrictions. After cancer cell capture, a reverse flow was used to retrieve the captured cancer cells from the device. Isolation efficiencies higher than 80% were achieved for breast and colon cancer cell lines. In addition, this device was able to successfully detect and retrieve CTCs from the peripheral blood of patients with metastatic lung cancer.

Hydrodynamic micro-filters based on cell size variations have also been developed for cancer cell separation. For example, Hur and Di Carlo *et al.* utilized microscale laminar vortices combined with inertial focusing to selectively isolate and trap larger cancer cells spiked into whole blood while smaller blood cells were flushed out of the device (see Fig. 3(c)).[75] Multiple microscale laminar vortices were created on chip with processing rates as high as $7.5 \times 10^6$ cells per second. The reported cell recovery rates for these devices were ~23% for MCF-7 cells and ~10% for HeLa cells.

## 5 On-chip DEP

Dielectrophoresis (DEP) uses the polarization of cells in non-uniform electrical fields to exert forces on cells. DEP forces depend on factors such as cell membrane and cytoplasm electrical properties as well as cell size.[123] A number of microfluidic

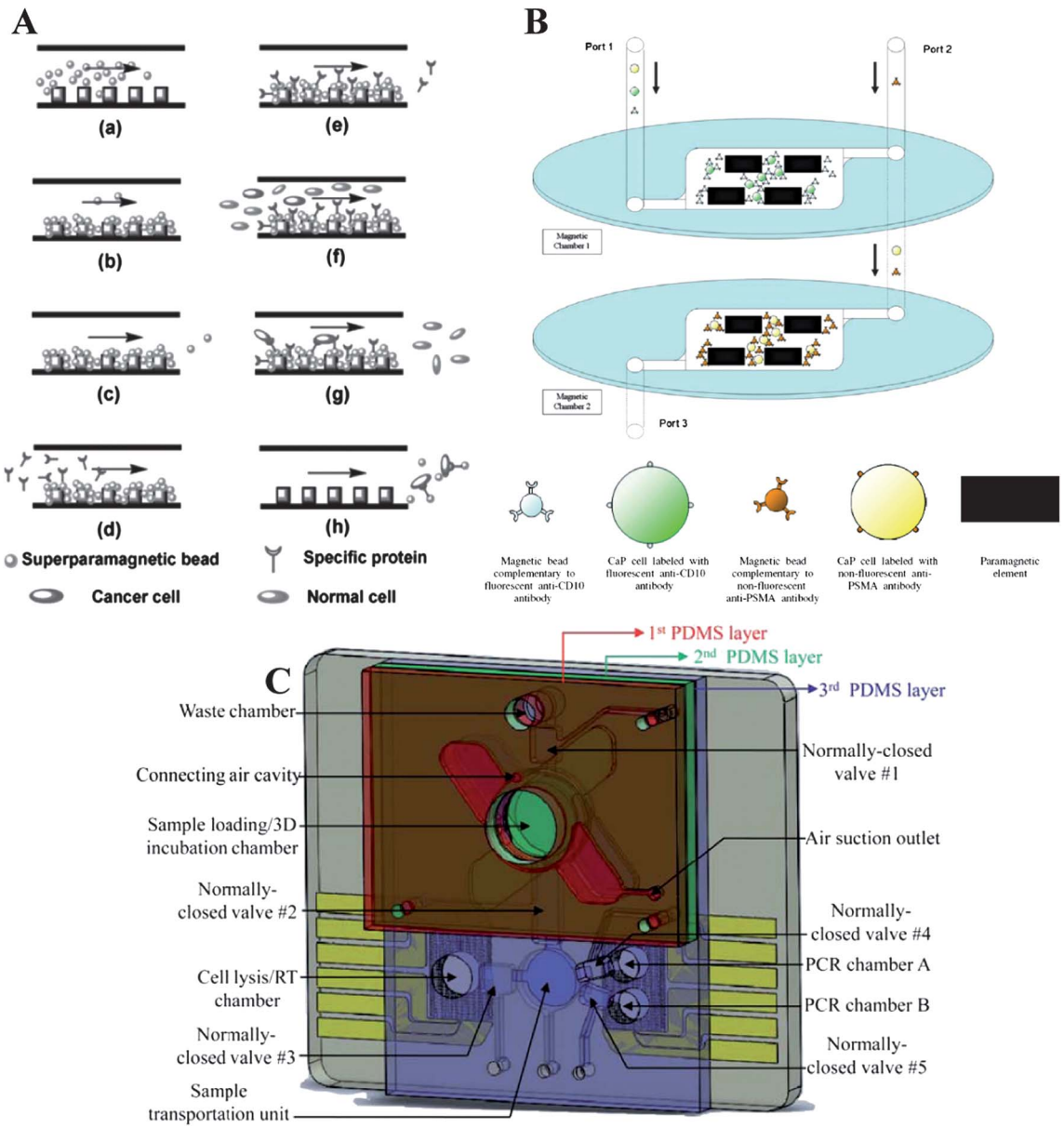


**Fig. 2** Magnetic activated micro-cell sorters. (a) Step by step illustration of the first magnetic activated micro-cell sorter for cancer cell capture. Reproduced with permission from ref. 55. (b) Schematic of a microfluidic device for serial selection of cellular subpopulations by the use of antibody-coated magnetic beads. Reproduced with permission from ref. 57. (c) An integrated magnetic-based cancer cell capture platform, consisting of an incubator for the magnetic beads to capture cancer cells, a control module for sample transportation, and a nucleic acid amplification module for cell lysis and genetic identification. Reproduced with permission from ref. 59.

DEP devices have been developed for separating cancer cells (see summary in Table 4), based on differences in cells' response to electric fields.[124–126] Becker and Gascoyne *et al.* reported the first dielectric affinity column (see Fig. 4(a)) for cancer cell separation in which human leukaemia cells suspended within normal blood cells were retained on microelectrode arrays while normal blood cells were eluted.[96] The cancer cells were subsequently released for collection by the removal of the DEP field. Becker and Gascoyne *et al.* further demonstrated the applicability of this method for the separation of epithelial cancer cells (MDA-231 cells) from diluted blood and reported a recovery rate of 95%.[97,98]

DEP affinity columns require the activation and deactivation of electric fields. To achieve continuous flow separation of cancer cells, Gascoyne *et al.* proposed DEP flow-field fractionation (DEP-FFF) wherein DEP forces are generated to levitate suspended cells to different equilibrium heights within a microfluidic chamber, based on variations of cells' electrical properties.[103] The levitated cells are transported at different flow velocities upon the application of fluid flow (see Fig. 4(b)). Using this approach, human leukemic (HL-60) cells,[99,106] MDA-435 cells,[101,102] MDA-468 cells and MDA-231 cells[113] were successfully separated from background cell populations. Furthermore, DEP-FFF was used to study the membrane capacitance, density, and hydrodynamic

 

**Table 3** Cell size-based cancer cell separation microfluidic devices

| Cell separation structures | Targeted cells | Carrier medium and control cells | Target cell recovery rate | Capture purity |
|---|---|---|---|---|
| Four successively narrower polyurethane channels[64] | Human neuroblastoma cells | Human whole blood or isolated mononuclear cells in PBS | NA | NA |
| Glass based pool and dam structures[65] | Human lung cancer cells of SPC-A-1 | Human blood from healthy donors ($10^6$ RBCs and $2 \times 10^5$ cancer cells) | 99.9% | NA |
| One-layer parylene-C membrane micro-filters [66] | Human prostate cancer cells of LNCaP | Human blood samples from healthy donors (50–500 cell per ml) | 89.5% ± 9.5% | NA |
| One-layer parylene-C membrane micro-filters[72] | Human breast cancer cells of MCF-7, SK-Br-3, and MDA-231, bladder cancer cells of J82, T24 and RT4 and prostate cancer cells of LNCaP | Human blood samples from healthy donors (5 cells per ml) | 96.5% (≥1 cells) and 64% (≥3 cells) | NA |
| One-layer parylene-C membrane micro-filters[72] | CTCs | Blood samples from patients with metastatic prostate, breast, colon, or bladder cancer | CTC identification in 51 of 57 patient samples | NA |
| 3D parylene-C membrane micro-filters[77] | Human prostate cancer cells of LNCaP and breast cancer cells of MCF-7 | Blood samples from health donors (~30 MCF-7 and ~100 LNCaP cells per ml) | 86.5% ± 5.3% | NA |
| PDMS based crescent shaped isolation wells[68] | Human breast and cancer cells of MCF-7 and MDA-231, colon cancer cells of HT-29 | Blood samples from healthy donors (100 cancer cells per ml) | >80% | >80% |
| PDMS based crescent shaped isolation wells[73] | Human breast cancer cells of MCF-7 and MDA-231, gastric cancer cells of AGS and N87, hepatocellular cancer cells of HepG2 and HuH7, tongue cancer cells of CAL27 and pharynx cancer cells of FADU | PBS and whole blood samples from healthy donors (100 cancer cells per ml) | ~80% | Mean value of 89% |
| PDMS based crescent shaped isolation wells[73] | CTCs | Blood samples from patients with metastatic lung cancer | CTC identification in 5 of 5 patient samples | Mean value of 83% |
| Size-selective micro-cavity arrays made of nickel[69] | Human lung cancer cells of NCI-H358, breast cancer cells of MCF-7, gastric cancer cells of AGS and SNU-1, and colon cancer cells of SW620 | Blood samples from healthy donors (10–100 cancer cells per ml) | >80% | NA |
| PDMS based dam structures + lectin cocanavalin A[71] | Human leukemic cells of K562 | Blood from healthy mice ($10^6$ RBCs and $2 \times 10^5$ K562 cells) | ~84% | NA |
| Polyurethane-methacrylate based lateral micro-filters with arrays of pillars[70] | Human breast cancer cells of MCF-7 (fixed and unfixed) | Blood samples from healthy donors | ~90% (fixed cancer cells) and ~50% (unfixed cells) | NA |
| Inertial flow in spiral micro-channels made of PDMS[67] | Human neuroblastoma cells of SH-SY5Y and rat glioma cells of C6 | PBS | ~80% | NA |
| PDMS based expansion–contraction reservoirs to produce micro-vortices[75] | Human cervical cancer cells of HeLa and breast cancer cells of MCF-7 | Blood samples containing leukocytes only (1 : 100 of cancer cells to leukocytes) | ~23% (MCF-7) and ~10% (HeLa) | 7.1-fold enrichment for MCF-7 and 5.5-fold enrichment for HeLa |
| PDMS based high aspect ratio rectangular micro-channels patterned with a contraction–expansion array[74] | Human breast cancer cells of MCF-7 | PBS and blood samples (500 MCF-7 cells per ml) | >90% (MCF-7 in PBS) and ~80% (MCF-7 in blood samples) | $3.3 \times 10^5$-fold enrichment over RBCs and $1.2 \times 10^4$-fold enrichment over leukocytes |

properties of cultured cancer cells. The results revealed that cancer cells' biophysical properties changed over time through a process of cytoplasmic shedding whereby cell membrane and cytoplasm were lost.[95]

To enhance sorting sensitivities, a 3D-asymmetric microelectrode setup was developed for cancer cell separation (see Fig. 4(c)).[108] Compared to conventional 3D-microelectrode systems, which feature constant electric field magnitudes, the 3D-asymmetric microelectrode system employed electric fields of continuously varying magnitudes along the transverse direction of a channel owing to variable electrode widths in the half-circular shaped cross-section of the microchannel. The varying dielectric forces enabled a higher sorting sensitivity, which was demonstrated by the separation of mouse P19 embryonic carcinoma from RBCs[108] and MCF-7 cells from healthy counterparts (MCF-10A).[112]

An alternative method for separating cancer cells has been demonstrated by combining multi-orifice flow fractionation

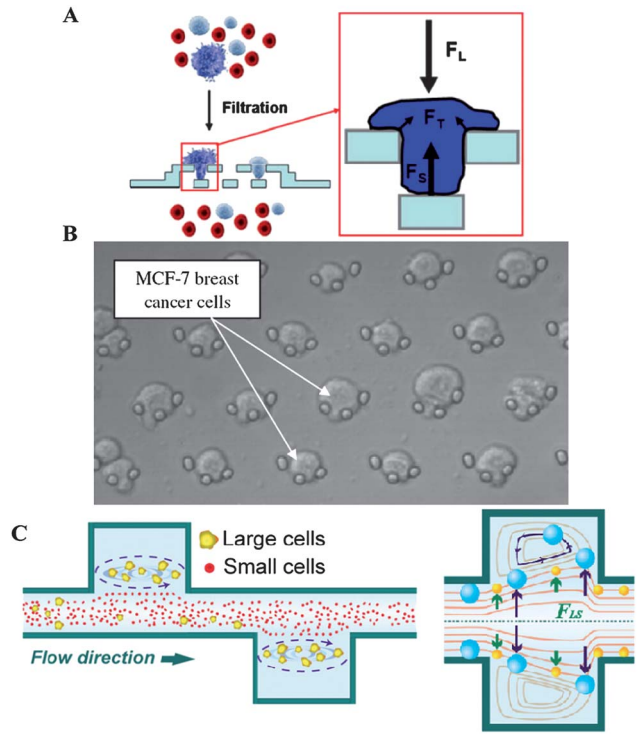


**Fig. 3** Microfluidic devices for cancer cell capture and separation based on cell size differences. (a) A 3D parylene membrane micro-filter, reproduced with permission from ref. 77. (b) A PDMS micro-filter with crescent-shaped isolation wells captured cancer cells, reproduced with permission from ref. 68. (c) A micro-device for trapping large cells and eluting small cells by combining microscale laminar vortices with inertial focusing, reproduced with permission from ref. 75.

(MOFF) with DEP.[76] As shown in Fig. 4(d), when cell samples were introduced through the inlet, most of the blood cells were separated *via* MOFF and extracted through outlet I while MCF-7 cells with residual blood cells (not fully separated) proceeded to the DEP separator. At the DEP separator, cancer cells exited through outlet II while the residual blood cells passed through outlet III. The serial combination of the two sorting techniques enabled high-speed, continuous flow-through separation without labelling, which recorded a 162-fold increase in MCF-7 cells at a flow rate of 126 ml $min^{-1}$ while RBCs and WBCs were efficiently removed with separation efficiencies of 99.24% and 94.23%, respectively.

## 6 Conclusion and outlook

This review summarized the working principles and experimental results of key microfluidic technologies for cancer cell separation and detection. These microfluidic devices are based on cell-affinity micro-chromatography, magnetic activated micro-cell sorting, size-based microfluidic separation, and dielectrophoresis. Despite the recent technological advances, the development of a single device capable of simultaneously achieving high throughput, high target cancer cell recovery, high purity, and high cell viability remains challenging.

A significant challenge for cell-affinity micro-chromatography and magnetic activated micro-cell sorting techniques is their low processing throughput. This is limited by the number of sufficient interactions between surface-bound ligands and target cancer cells. Although various capture structures such as micro-posts,[39,44] 3D nano-structures,[43,49] and patterned herringbones[45] have been shown to increase these interactions, current device throughputs remain within millilitres per hour.[33] While these techniques permit reasonably high cancer cell capture purity by using highly selective antibodies or aptamers (*e.g.*, capture purity of 62% ± 2% for prostate cancer CTC capture purity from patient samples[44]), non-specific absorption of cells onto device surfaces must be better overcome before capture purity can be further improved.

Compared to affinity-based techniques, micro-filtration methods have a higher throughput as these methods are compatible with higher flow rates. For example, hydrodynamic micro-filters[75] were reported to process $7.5 \times 10^6$ cells per second. Micro-filters also enable higher capture purity of CTCs compared to affinity-based techniques due to the significant size and deformability differences between CTCs and blood cells (*e.g.*, CTC capture purity of ~83% from human samples using micro-filters[73]). However, these methods suffer from low cell viability resulting from potential damage incurred as the cells pass through narrow filter pores, which renders the use of micro-filters less compatible for live cell interrogations (*e.g.*, cell suspensions were partially fixed before being passed through a membrane micro-filter[72]).

Since the DEP technique leverages differences in both cellular size and dielectric properties, it could potentially lead to a higher cancer cell separation yield and purity compared to micro-filtration methods that are based on cell size differences only. However, in practice, due to the limited dielectric differences between target cells and carrier cells, this technique's yield and purity are not as high as expected (see summary in Table 4). Furthermore, most of the reported on-chip DEP separation microfluidic devices require the use of a low conductivity medium (*e.g.*, sucrose solution[96,97,117]). Thus, cell viability after DEP separation is also a concern. Among the detection techniques discussed in this review, on-chip DEP is the only technique that has not yet undergone verifications with clinical samples.

Thus, an approach that utilizes a combination of multiple cell-capture methods may prove viable for improving the performance of cancer cell capture devices. For example, to improve device selectivity and cell-capture efficiency, one may envision a multi-module microfluidic system for cancer cell capture in which the first module performs high-throughput concentration and purification of target cells while a second module enables the selective capture of cancer cells. Such a device can be realized by integrating DEP with cell affinity micro-chromatography, such as for CTC detection. The DEP module would function as a pre-concentrator to increase the concentration of CTCs by flushing samples through channels patterned with electrodes. The concentrated samples would then enter the cell affinity micro-chromatography module for high-purity CTC capture.

While the majority of existing systems focused on cell capture alone, integrated microfluidic systems capable of both cancer cell capture and post-capture processing have attractive prospects. One such system, based on cell affinity micro-chromatography, enables both selective cancer cell capture and post-capture

**Table 4** DEP-based cancer cell separation microfluidic devices

| Cell separation structures | Targeted cells | Carrier medium and control cells | Target cell recovery rate | Capture purity |
|---|---|---|---|---|
| An electrode affinity column with interdigitated micro-electrodes[96] | Human leukemic cells of HL-60 | Blood cells + sucrose solution | NA | ~80% (initial mixture of $2 \times 10^7$ HL-60 and $3 \times 10^7$ blood cells) |
| A dielectric affinity column with interdigitated micro-electrodes[97] | Human breast cancer cells of MDA-231 | Blood samples + sucrose solution | NA | ~95% (initial mixture of $1 \times 10^7$ MDA-231 and $3 \times 10^7$ blood cells) |
| A dielectric affinity column with an interdigitated micro-electrodes[98] | Human breast cancer cells of MDA-231 | Blood samples + sucrose solution | >95% | NA |
| A dielectric affinity column with reconfigurable electrodes[100] | Human cervical cancer cells of HeLa | Human peripheral blood cells + sucrose solution | NA | NA |
| A dielectric affinity column with a micro-electrode array[104] | Human monocytic cells of U937, lymphoma cells of Jurkat, HTLV-1, tax-transformed human T cells of Ind-2, glioma cells of HTB, and neuroblastoma cells of SH-SY5Y | Peripheral blood mononuclear cells + sucrose solution | 47%–79% | >95% |
| DEP field flow fraction with interdigitated electrodes[99] | Human leukemic cells of HL-60 | WBCs from blood samples + sucrose solution | NA | NA |
| DEP field flow fraction with interdigitated electrodes[101] | Human breast cancer cells of MDA-435 | Hematopoietic CD34+ stem cells + sucrose solution | NA | >99% (initial MDA-435 : stem cells = 2 : 3) |
| DEP field flow fraction with interdigitated electrodes[102] | Human breast cancer cells of MDA-435 | Blood samples + sucrose solution | NA | >98% of MDA-435 (initial MDA-435 : blood cells = 2 : 3) |
| DEP field flow fraction with interdigitated electrodes[113] | Human breast cancer cells of MDA-435, MDA-468 and MDA-231 | Peripheral blood mononuclear cells + sucrose solution | >90% | NA |
| Microscope slides coated with electrode arrays with changing frequencies[106] | Human breast cancer cells of MDA-435 and leukemic cells of HL-60 | Blood samples + sucrose | NA | NA |
| Microscope slides coated with electrode arrays with changing frequencies[110] | Cancer cells from biopsy | Biopsied cells + sucrose solution | NA | NA |
| 3D-asymmetric micro-electrodes with a continuously varied electric field[108] | Mouse P19 embryonic carcinoma cells | Mouse RBCs + PBS | NA | 81.5% ± 7.6% of P19 EC and 94.1% ± 4.3% RBCs (initial ratio 1 : 1) |
| 3D-asymmetric micro-electrodes with a continuously varied electric field[112] | Human breast cancer cells of MCF-7 and MCF-10A | PBS | 86.67% of MCF-7 and 98.73% of MCF-10A | NA |
| DC-dielectrophoresis[111] | Fixed WBCs and human breast cancer cells of MCF-7 | Trehalose solution | NA | NA |
| Guided DEP with a pair of planar electrodes[114] | Human leukemic cells of Jurkat and cervical cancer cells of HeLa | Sucrose solution | NA | NA |
| Planar interdigitated microelectrodes[115] | Clones of mouse melanoma B16F10 cells | Sucrose solution | NA | NA |
| A planar electrode pair with an angle to the flow direction[116] | Human colorectal cancer cells of HCT116 and embryonic kidney cells of HEK 293 | PBS | NA | 95% of HCT116 |
| Interdigitated comb-like electrodes for DEP based deflection[117] | Human breast cancer cells of MDA-231 | Sucrose solution | 96% ± 1.15% | NA |
| Combination of multi-orifice flow fractionation and DEP[76] | Human breast cancer cells of MCF-7, RBCs and WBCs | Sucrose and PBS | 75.18% | 162-fold increase in MCF-7 cells |



processing (release of captured cancer cells and subsequent enumeration, manipulation, and molecular identification).[47,51] However, further research is required to improve the retrieval of captured cancer cells from this system as the shear stresses and enzymes used to detach the captured cells may harm them and alter the cellular characteristics.[47]

In contrast to cell affinity micro-chromatography, magnetic activated cell sorting readily permits the manipulation of captured cancer cells by controlling local magnetic fields for post-capture processing. Lien and Lee *et al.* proposed a multi-functional, integrated magnetic bead-based microfluidic device capable of cancer cell separation, cell lysis, and

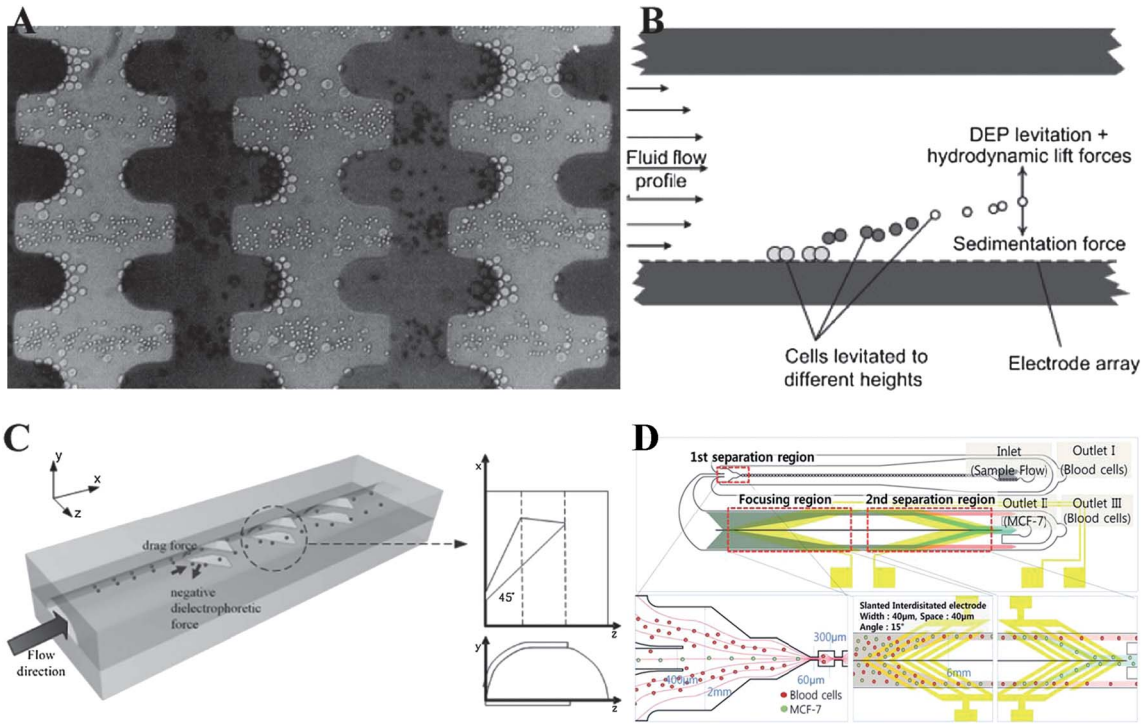


**Fig. 4** Microfluidic DEP devices for cancer cell separation. (a) A dielectric affinity column for cancer cell separation where large cancer cells are trapped on electrode tips while small blood cells are eluted. Reproduced with permission from ref. 97. (b) DEP-FFF combines DEP, sedimentation and hydrodynamic forces to influence cell positions in the hydrodynamic flow profile. Reproduced with permission from ref. 113. (c) A 3D-asymmetric microelectrode system for DEP cell separation, reproduced with permission from ref. 108. (d) A continuous separator integrates multi-orifice flow fractionation and DEP. Reproduced with permission from ref. 76.

genetic identification.[59] Microfiltration methods also permit easy retrieval of captured cancer cells, as demonstrated by Tan and Lim *et al.*, using a reverse flow to release captured cancer cells in multiple arrays of crescent-shaped wells.[68,73] However, on-chip post-capture processing capabilities have yet to be developed.

Microfluidic devices capable of measuring cellular biophysical properties can also prove useful for cancer cell detection. A few microfluidic devices have been developed to measure single cell mechanical[127–132] and/or electrical properties,[133–136] enabling the discrimination of normal cells from malignant counterparts (summary in Table 5). For example, Guck *et al.* developed a microfluidic optical stretcher for cancer cell mechanical characterization (see Fig. 5(a)), indicating that cells with higher metastatic potentials (*e.g.*, Mod-MCF-7) deformed more than normal cells (*e.g.*, MCF-10).[80,81] Hou and Lim *et al.* quantified the time required for cells to deform and pass through a narrow constriction channel where MCF-10A cells were found to have longer entry time and higher stiffness as compared to MCF-7 cells of similar sizes.[83] Chen and Sun *et al.* used a microfluidic device to electrodeform single cells, reporting different Young's modulus values of two cervical cancer cells having different metastatic pathways (SiHa *vs.* ME180).[84]

For electrical characterization of cells, Labeed and Hughes *et al.* pioneered the use of DEP to determine the electrical property differences in cancer cells with and without drug treatment, for instance, K562AR *vs.* K562[87] and parental MCF-7 cells *vs.* drug resistant derivatives including MCF-7TaxR, MCF-7DoxR and MCF-7MDR.[93] Han *et al.* presented the first application of micro-electrical impedance spectroscopy in cancer cell classification by reporting significant impedance differences among breast cancer cell lines (MCF-7, MDA-231, MDA-435, and MCF-10A)[118] and head-and-neck cancer cell lines with different metastatic potentials (686LN *vs.* 686LN-M4e).[119] Furthermore, Chen and Sun reported a microfluidic system for cell type classification using both mechanical and electrical parameters of cells (see Fig. 5(b)), demonstrating that electrical and mechanical parameters, when used in combination, can provide a higher cell classification success rate in distinguishing EMT6 (murine breast cancer cell lines) from its multi-drug resistant counterpart EMT6/AR1.0.[85]

A challenge for microfluidic cancer cell biophysical characterization is existing devices' low sample throughput. To obtain clinically relevant information, these devices must be able to measure biophysical properties of a large number of cells with true high throughputs. However, existing systems are only capable of processing small numbers of cells within a reasonable time frame. For example, the total number of cells tested by the optical stretcher was 36 for MCF-10, 26 for MCF-7, and 21 for Mod-MCF-7.[81] Reported electrical impedance spectroscopy differences of head-and-neck cancer cell lines with different metastatic potentials (686LN *vs.* 686LN-M4e) were also based on the testing of low sample numbers ($n = 72$ for the 686LN-M4e cell and $n = 57$ for the 686LN cell).[119] Furthermore, most microfluidic devices to date are only capable of characterizing a single biophysical parameter. Future development of systems

 

**Table 5** Microfluidic devices for cancer cell biophysical property characterization

| Techniques | Cell lines | Key observations |
|---|---|---|
| DEP | Human leukemic cells of K562 and its doxorubicin-resistant counterpart (K562AR) | Compared to K562, K562AR cells show one fold higher in cytoplasm conductivity and comparable specific membrane capacitance[87] |
| DEP | Human leukemic cells of Daudi and NCI-H929 | The specific membrane capacitance for nonviable cancer cells is one order lower than viable counterparts[88] |
| DEP | Human leukemic cells (K562) treated with staurosporine | After drug treatment, there is an increase in both specific membrane capacitance and cytoplasm conductivity of K562 cells[90,91] |
| DEP | Human oral squamous carcinoma cells of H357 and HPV-16 transformed keratinocyte cells of UP | Compared to benign cells of UP, malignant cells of H357 have a lower cytoplasm conductivity and a higher specific membrane capacitance[92] |
| DEP | Human breast cancer cells of MCF-7 and its multiple drug resistant derivatives | There are significant changes in their cytoplasm conductivities: MCF-7TaxR < MCF-7 < MCF-7MDR1 < MCF-7DoxR[93] |
| DEP | Human leukemic cells of K562 and its doxorubicin-resistant counterpart (K562AR) treated with ion channel blockers | There is a significant decrease in cytoplasm conductivity for K562AR cells treated with ion channel blockers while the effect of these drugs on K562 cells is negligible[94] |
| DEP | Human breast cancer cells of MDA-435 and MDA-231 as well as primary human cancer cells | Following dissociation from their growth sites, the physical characteristics of cancer cells are shown to differ from those of blood cells[95] |
| Electrorotation | Human breast cancer cells of MDA-231, lymphocytes and erythrocytes | Dielectric differences (*e.g.*, membrane specific capacitance and cytoplasm conductivity) between cancer cells and blood cells are recorded[97] |
| Electrorotation | Human breast cancer cells of MCF/neo, MCF/HER2–11 and MCF/HER2–18 | Variations in dielectric properties among breast cancer cells in their levels of p185neu expression are detected[138] |
| Optical stretcher | Human breast cancer cells of MCF-10, MCF-7, and Mod-MCF-7 with higher metastatic potential | Cells with higher metastatic potentials stretch significantly more than normal cells[80] |
| Optical stretcher | Human breast cancer cells of MCF-7, Mod-MCF-7, MCF-10A, MDA-231 and mod MDA-MB-231 | Cells with higher metastatic potentials stretch significantly more than normal cells[81] |
| Flat or nanostructured surfaces | Human breast cancer cells of MCF-7 and MCF-10A | MCF-10A cells demonstrate higher adhesion than MCF7 cells regardless of culture time and surface nanotopography[78] |
| Bulge generation | Human breast cancer cells of MCF-7 and MCF-10A | The bulges generated in MCF-7 cells are not evenly distributed as in MCF-10A cells. The morphologies of bulges of MCF-7 and MCF10-A cells are swollen protrusion and tubular protrusion, respectively[82] |
| Constriction channel | Human breast cancer cells of MCF-7 and MCF-10A | Benign cells have longer entry time and a higher stiffness than malignant counterparts of similar sizes[83] |
| Electrodeformation | Human cervical cancer cells of SiHa and ME180 | Two cervical cancer cells with different metastatic pathways have different Young's modulus values[84] |
| Impedance spectroscopy | Human breast cancer cells of MCF-7, MDA-231, MDA-435 and MCF-10A | Impedance differences are recorded among different breast cancer cells[118] |
| Impedance spectroscopy | Human head and neck cancer cells of 686LN and 686LN-M4e | Impedance differences are recorded between head and neck cancer cells with different metastatic potential[119] |
| Impedance spectroscopy | Human oral cancer cells of CAL 27 and non-cancer oral epithelial cells of Het-1A | At equal cell number, cancer cells generate impedance several folds higher than that of non-cancer cells[120,121] |
| Impedance spectroscopy and constriction channel | Murine breast cancer cells of EMT6 and its multiple drug resistant counterpart EMT6/AR1.0 | Differences in both electrical parameters of impedance spectroscopy and mechanical properties of transit time are recorded from cancer cells with and without multiple drug resistance[85] |



that are capable of measuring multiple biophysical parameters will be important for accuracy improvement.

In summary, the microfluidic environment allows for unprecedented spatio-temporal control of cells. While the development of microfluidic devices for cancer detection is relatively recent, a number of studies have demonstrated microfluidic devices' feasibility in isolating and identifying cancer cells from clinical samples (*e.g.*, cell-affinity chromatography,[39,41,44,45] magnetic activated cell sorting,[60] and micro-filtration methods[72,73]). The next few years will witness even more intense development of innovative microfluidic systems for cancer cell detection, characterization, and separation. Cells in patient samples are extremely heterogeneous, making the detection of cancer cells an inherently multi-dimensional problem. Overcoming these challenges requires the development of combinatorial systems that take advantage of the multiple unique properties of cancer cells

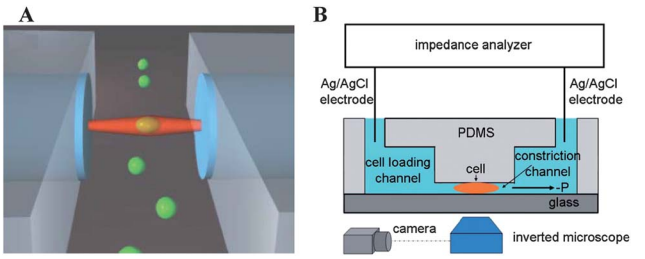


**Fig. 5** Microfluidic devices for electrical and mechanical property characterization of cancer cells. (a) Optically induced forces lead to trapping and stretching of cells with two counter propagating divergent laser beams. Reproduced with permission from ref. 81. (b) A microfluidic system for simultaneously electrical and mechanical characterization of single cells using impedance spectroscopy and constriction channel. Reproduced with permission from ref. 85.

(*e.g.*, surface antigens as well as biophysical properties) for cancer cell identification and isolation. The next generation of microfluidic devices would possibly make use of multiple biochemical and biophysical cues that are unique to cancer cells to achieve high cancer cell capture purity and recovery, high cell viability, and high throughput, which would enhance the clinical relevance of microfluidic technologies for cancer detection.

## Acknowledgements

This work was supported by the Natural Sciences and Engineering Research Council of Canada (NSERC) under the Strategic Project Grants program and by the Canada Research Chairs Program.

## References

1 R. W. Ruddon and Ebrary Inc., *Cancer Biology*, Oxford University Press, New York, 3rd edn, 2007.
2 A. Jemal, R. Siegel, J. Q. Xu and E. Ward, Cancer statistics, 2010, *Ca-Cancer J. Clin.*, 2010, **60**, 277–300.
3 P. Bannasch, *Cancer Diagnosis: Early Detection*, Springer, Berlin, New York, 1992.
4 J. M. Elwood and S. B. Sutcliffe, *Cancer Control*, Oxford University Press, Oxford, New York, 2010.
5 W. E. O'Donnell, in *Early Detection and Diagnosis of Cancer*, ed. W. E. O'Donnell, E. Day and L. Venet, C.V. Mosby Co., Saint Louis, 1962.
6 M. Verma, B. K. Dunn, A. Umar, New York Academy of Sciences and National Cancer Institute (U.S.), Division of Cancer Prevention, *Epigenetics in Cancer Prevention: Early Detection and Risk Assessment*, New York Academy of Sciences, New York, 2003.
7 A. Armakolas, Z. Panteleakou, A. Nezos, A. Tsouma, M. Skondra, P. Lembessis, N. Pissimissis and M. Koutsilieris, Detection of the circulating tumor cells in cancer patients, *Future Oncol.*, 2010, **6**, 1849–1856.
8 M. Danova, M. Torchio and G. Mazzini, Isolation of rare circulating tumor cells in cancer patients: technical aspects and clinical implications, *Expert Rev. Mol. Diagn.*, 2011, **11**, 473–485.
9 S. I. Kim and H. Jung, Circulating tumor cells: detection methods and potential clinical application in breast cancer, *J. Breast Cancer*, 2010, **13**, 125–131.
10 M. Yu, S. Stott, M. Toner, S. Maheswaran and D. A. Haber, Circulating tumor cells: approaches to isolation and characterization, *J. Cell Biol.*, 2011, **192**, 373–382.
11 V. Zieglschmid, C. Hollmann and O. Bocher, Detection of disseminated tumor cells in peripheral blood, *Crit. Rev. Clin. Lab. Sci.*, 2005, **42**, 155–196.
12 T. M. Squires and S. R. Quake, Microfluidics: fluid physics at the nanoliter scale, *Rev. Mod. Phys.*, 2005, **77**, 977.
13 G. M. Whitesides, The origins and the future of microfluidics, *Nature*, 2006, **442**, 368–373.
14 H. Andersson and A. van den Berg, Microfluidic devices for cellomics: a review, *Sens. Actuators, B*, 2003, **92**, 315–325.
15 N. Li, A. Tourovskaia and A. Folch, Biology on a Chip: Microfabrication for Studying the Behavior of Cultured Cells, *Critical Review in Biomedical Engineering*, 2003, vol. 31, pp. 423–488.
16 T. H. Park and M. L. Shuler, Integration of cell culture and microfabrication technology, *Biotechnol. Prog.*, 2003, **19**, 243–253.
17 C. Q. Yi, C. W. Li, S. L. Ji and M. S. Yang, Microfluidics technology for manipulation and analysis of biological cells, *Anal. Chim. Acta*, 2006, **560**, 1–23.
18 Y. Tanaka, K. Sato, T. Shimizu, M. Yamato, T. Okano and T. Kitamori, Biological cells on microchips: new technologies and applications, *Biosens. Bioelectron.*, 2007, **23**, 449–458.
19 A. L. Paguirigan and D. J. Beebe, Microfluidics meet cell biology: bridging the gap by validation and application of microscale techniques for cell biological assays, *BioEssays*, 2008, **30**, 811–821.
20 J. W. Warrick, W. L. Murphy and D. J. Beebe, Screening the cellular microenvironment: a role for microfluidics, *IEEE Reviews in Biomedical Engineering*, 2008, **1**, 75–93.
21 G. Velve-Casquillas, M. Le Berre, M. Piel and P. T. Tran, Microfluidic tools for cell biological research, *Nano Today*, 2010, **5**, 28–47.
22 D. Wlodkowic and J. M. Cooper, Tumors on chips: oncology meets microfluidics, *Curr. Opin. Chem. Biol.*, 2010, **14**, 556–567.
23 D. Wlodkowic and J. M. Cooper, Microfabricated analytical systems for integrated cancer cytomics, *Anal. Bioanal. Chem.*, 2010, **398**, 193–209.
24 D. Wlodkowic and J. M. Cooper, Microfluidic cell arrays in tumor analysis: new prospects for integrated cytomics, *Expert Rev. Mol. Diagn.*, 2010, **10**, 521–530.
25 E. W. K. Young and D. J. Beebe, Fundamentals of microfluidic cell culture in controlled microenvironments, *Chem. Soc. Rev.*, 2010, **39**, 1036–1048.
26 P. R. C. Gascoyne and J. Vykoukal, Particle separation by dielectrophoresis, *Electrophoresis*, 2002, **23**, 1973–1983.
27 C. F. Gonzalez and V. T. Remcho, Harnessing dielectric forces for separations of cells, fine particles and macromolecules, *J. Chromatogr., A*, 2005, **1079**, 59–68.
28 M. Radisic, R. K. Iyer and S. K. Murthy, Micro- and nanotechnology in cell separation, *Int. J. Nanomed.*, 2006, **1**, 3–14.
29 C. X. Liu, T. Stakenborg, S. Peeters and L. Lagae, Cell manipulation with magnetic particles toward microfluidic cytometry, *J. Appl. Phys.*, 2009, **105**, 102014.
30 A. A. S. Bhagat, H. Bow, H. W. Hou, S. J. Tan, J. Han and C. T. Lim, Microfluidics for cell separation, *Med. Biol. Eng. Comput.*, 2010, **48**, 999–1014.
31 T. F. Didar and M. Tabrizian, Adhesion based detection, sorting and enrichment of cells in microfluidic Lab-on-Chip devices, *Lab Chip*, 2010, **10**, 3043–3053.
32 D. R. Gossett, W. M. Weaver, A. J. Mach, S. C. Hur, H. T. K. Tse, W. Lee, H. Amini and D. Di Carlo, Label-free cell separation and sorting in microfluidic systems, *Anal. Bioanal. Chem.*, 2010, **397**, 3249–3267.
33 U. Dharmasiri, M. A. Witek, A. A. Adams and S. A. Soper, Microsystems for the capture of low-abundance cells, *Annu. Rev. Anal. Chem.*, 2010, **3**, 409–431.
34 E. D. Pratt, C. Huang, B. G. Hawkins, J. P. Gleghorn and B. J. Kirby, Rare cell capture in microfluidic devices, *Chem. Eng. Sci.*, 2011, **66**, 1508–1522.
35 M. Zborowski and J. J. Chalmers, Rare cell separation and analysis by magnetic sorting, *Anal. Chem.*, 2011, **83**, 8050–8056.
36 Z. Du, N. Colls, K. H. Cheng, M. W. Vaughn and L. Gollahon, Microfluidic-based diagnostics for cervical cancer cells, *Biosens. Bioelectron.*, 2006, **21**, 1991–1995.
37 S. P. Wankhede, Z. Du, J. M. Berg, M. W. Vaughn, T. Dallas, K. H. Cheng and L. Gollahon, Cell detachment model for an antibody-based microfluidic cancer screening system, *Biotechnol. Prog.*, 2006, **22**, 1426–1433.
38 Z. Du, K. H. Cheng, M. W. Vaughn, N. L. Collie and L. S. Gollahon, Recognition and capture of breast cancer cells

using an antibody-based platform in a microelectromechanical systems device, *Biomed. Microdevices*, 2007, **9**, 35–42.
39 S. Nagrath, L. V. Sequist, S. Maheswaran, D. W. Bell, D. Irimia, L. Ulkus, M. R. Smith, E. L. Kwak, S. Digumarthy, A. Muzikansky, P. Ryan, U. J. Balis, R. G. Tompkins, D. A. Haber and M. Toner, Isolation of rare circulating tumour cells in cancer patients by microchip technology, *Nature*, 2007, **450**, 1235–1239.
40 A. A. Adams, P. I. Okagbare, J. Feng, M. L. Hupert, D. Patterson, J. Gottert, R. L. McCarley, D. Nikitopoulos, M. C. Murphy and S. A. Soper, Highly efficient circulatingtumor cell isolation from whole blood and label-free enumeration using polymer-based microfluidics with an integrated conductivity sensor, *J. Am. Chem. Soc.*, 2008, **130**, 8633–8641.
41 S. Maheswaran, L. V. Sequist, S. Nagrath, L. Ulkus, B. Brannigan, C. V. Collura, E. Inserra, S. Diederichs, A. J. Iafrate, D. W. Bell, S. Digumarthy, A. Muzikansky, D. Irimia, J. Settleman, R. G. Tompkins, T. J. Lynch, M. Toner and D. A. Haber, Detection of mutations in EGFR in circulating lung-cancer cells, *N. Engl. J. Med.*, 2008, **359**, 366–377.
42 L. S. L. Cheung, X. G. Zheng, A. Stopa, J. C. Baygents, R. Guzman, J. A. Schroeder, R. L. Heimark and Y. Zohar, Detachment of captured cancer cells under flow acceleration in a bio-functionalized microchannel, *Lab Chip*, 2009, **9**, 1721–1731.
43 S. T. Wang, H. Wang, J. Jiao, K. J. Chen, G. E. Owens, K. I. Kamei, J. Sun, D. J. Sherman, C. P. Behrenbruch, H. Wu and H. R. Tseng, Three-dimensional nanostructured substrates toward efficient capture of circulating tumor cells, *Angew. Chem., Int. Ed.*, 2009, **48**, 8970–8973.
44 J. P. Gleghorn, E. D. Pratt, D. Denning, H. Liu, N. H. Bander, S. T. Tagawa, D. M. Nanus, P. A. Giannakakou and B. J. Kirby, Capture of circulating tumor cells from whole blood of prostate cancer patients using geometrically enhanced differential immunocapture (GEDI) and a prostate-specific antibody, *Lab Chip*, 2010, **10**, 27–29.
45 S. L. Stott, C. H. Hsu, D. I. Tsukrov, M. Yu, D. T. Miyamoto, B. A. Waltman, S. M. Rothenberg, A. M. Shah, M. E. Smas, G. K. Korir, F. P. Floyd, A. J. Gilman, J. B. Lord, D. Winokur, S. Springer, D. Irimia, S. Nagrath, L. V. Sequist, R. J. Lee, K. J. Isselbacher, S. Maheswaran, D. A. Haber and M. Toner, Isolation of circulating tumor cells using a microvortex-generating herringbone-chip, *Proc. Natl. Acad. Sci. U. S. A.*, 2010, **107**, 18392–18397.
46 B. Thierry, M. Kurkuri, J. Y. Shi, L. E. Lwin and D. Palms, Herceptin functionalized microfluidic polydimethylsiloxane devices for the capture of human epidermal growth factor receptor 2 positive circulating breast cancer cells, *Biomicrofluidics*, 2010, **4**, 32205.
47 U. Dharmasiri, S. K. Njoroge, M. A. Witek, M. G. Adebiyi, J. W. Kamande, M. L. Hupert, F. Barany and S. A. Soper, High-throughput selection, enumeration, electrokinetic manipulation, and molecular profiling of low-abundance circulating tumor cells using a microfluidic system, *Anal. Chem.*, 2011, **83**, 2301–2309.
48 M. D. Kurkuri, F. Al-Ejeh, J. Y. Shi, D. Palms, C. Prestidge, H. J. Griesser, M. P. Brown and B. Thierry, Plasma functionalized PDMS microfluidic chips: towards point-of-care capture of circulating tumor cells, *J. Mater. Chem.*, 2011, **21**, 8841–8848.
49 S. T. Wang, K. Liu, J. A. Liu, Z. T. F. Yu, X. W. Xu, L. B. Zhao, T. Lee, E. K. Lee, J. Reiss, Y. K. Lee, L. W. K. Chung, J. T. Huang, M. Rettig, D. Seligson, K. N. Duraiswamy, C. K. F. Shen and H. R. Tseng, Highly efficient capture of circulating tumor cells by using nanostructured silicon substrates with integrated chaotic micromixers, *Angew. Chem., Int. Ed.*, 2011, **50**, 3084–3088.
50 X. Zheng, L. S. Cheung, J. A. Schroeder, L. Jiang and Y. Zohar, A high-performance microsystem for isolating circulating tumor cells, *Lab Chip*, 2011, **11**, 3269–3276.
51 U. Dharmasiri, S. Balamurugan, A. A. Adams, P. I. Okagbare, A. Obubuafo and S. A. Soper, Highly efficient capture and enumeration of low abundance prostate cancer cells using prostate-specific membrane antigen aptamers immobilized to a polymeric microfluidic device, *Electrophoresis*, 2009, **30**, 3289–3300.
52 J. A. Phillips, Y. Xu, Z. Xia, Z. H. Fan and W. H. Tan, Enrichment of cancer cells using aptamers immobilized on a microfluidic channel, *Anal. Chem.*, 2009, **81**, 1033–1039.
53 Y. Xu, J. A. Phillips, J. Yan, Q. Li, Z. H. Fan and W. Tan, Aptamer-based microfluidic device for enrichment, sorting, and detection of multiple cancer cells, *Anal. Chem.*, 2009, **81**, 7436–7442.
54 K. H. Han, A. Han and A. B. Frazier, Microsystems for isolation and electrophysiological analysis of breast cancer cells from blood, *Biosens. Bioelectron.*, 2006, **21**, 1907–1914.
55 Y. J. Liu, S. S. Guo, Z. L. Zhang, W. H. Huang, D. Baigl, M. Xie, Y. Chen and D. W. Pang, A micropillar-integrated smart microfluidic device for specific capture and sorting of cells, *Electrophoresis*, 2007, **28**, 4713–4722.
56 M. G. Mauk, B. L. Ziober, Z. Y. Chen, J. A. Thompson and H. H. Bau, Lab-on-a-chip technologies for oral-based cancer screening and diagnostics—capabilities, issues, and prospects, *Ann. N. Y. Acad. Sci.*, 2007, **1098**, 467–475.
57 M. D. Estes, B. Ouyang, S. M. Ho and C. H. Ahn, Isolation of prostate cancer cell subpopulations of functional interest by use of an on-chip magnetic bead-based cell separator, *J. Micromech. Microeng.*, 2009, **19**, 095015.
58 H. Lee, T. J. Yoon, J. L. Figueiredo, F. K. Swirski and R. Weissleder, Rapid detection and profiling of cancer cells in fine-needle aspirates, *Proc. Natl. Acad. Sci. U. S. A.*, 2009, **106**, 12459–12464.
59 K. Y. Lien, Y. H. Chuang, L. Y. Hung, K. F. Hsu, W. W. Lai, C. L. Ho, C. Y. Chou and G. B. Lee, Rapid isolation and detection of cancer cells by utilizing integrated microfluidic systems, *Lab Chip*, 2010, **10**, 2875–2886.
60 A. E. Saliba, L. Saias, E. Psychari, N. Minc, D. Simon, F. C. Bidard, C. Mathiot, J. Y. Pierga, V. Fraisier, J. Salamero, V. Saada, F. Farace, P. Vielh, L. Malaquin and J. L. Viovy, Microfluidic sorting and multimodal typing of cancer cells in self-assembled magnetic arrays, *Proc. Natl. Acad. Sci. U. S. A.*, 2010, **107**, 14524–14529.
61 V. Sivagnanam, B. Song, C. Vandevyver, J. C. Bunzli and M. A. Gijs, Selective breast cancer cell capture, culture, and immunocytochemical analysis using self-assembled magnetic bead patterns in a microfluidic chip, *Langmuir*, 2010, **26**, 6091–6096.
62 K. Zhang, L. B. Zhao, S. S. Guo, B. X. Shi, T. L. Lam, Y. C. Leung, Y. Chen, X. Z. Zhao, H. L. W. Chan and Y. Wang, A microfluidic system with surface modified piezoelectric sensor for trapping and detection of cancer cells, *Biosens. Bioelectron.*, 2010, **26**, 935–939.
63 C. L. Chen, K. C. Chen, Y. C. Pan, T. P. Lee, L. C. Hsiung, C. M. Lin, C. Y. Chen, C. H. Lin, B. L. Chiang and A. M. Wo, Separation and detection of rare cells in a microfluidic disk *via* negative selection, *Lab Chip*, 2011, **11**, 474–483.
64 H. Mohamed, L. D. McCurdy, D. H. Szarowski, S. Duva, J. N. Turner and M. Caggana, Development of a rare cell fractionation device: application for cancer detection, *IEEE Trans. NanoBiosci.*, 2004, **3**, 251–256.
65 Z. Z. Chen, S. Y. Zhang, Z. M. Tang, P. F. Xiao, X. Y. Guo and Z. H. Lu, Pool-dam structure based microfluidic devices for filtering tumor cells from blood mixtures, *Surf. Interface Anal.*, 2006, **38**, 996–1003.
66 S. Zheng, H. Lin, J. Q. Liu, M. Balic, R. Datar, R. J. Cote and Y. C. Tai, Membrane microfilter device for selective capture, electrolysis and genomic analysis of human circulating tumor cells, *J. Chromatogr., A*, 2007, **1162**, 154–161.
67 S. S. Kuntaegowdanahalli, A. A. S. Bhagat, G. Kumar and I. Papautsky, Inertial microfluidics for continuous particle separation in spiral microchannels, *Lab Chip*, 2009, **9**, 2973–2980.
68 S. J. Tan, L. Yobas, G. Y. H. Lee, C. N. Ong and C. T. Lim, Microdevice for the isolation and enumeration of cancer cells from blood, *Biomed. Microdevices*, 2009, **11**, 883–892.
69 M. Hosokawa, T. Hayata, Y. Fukuda, A. Arakaki, T. Yoshino, T. Tanaka and T. Matsunaga, Size-selective microcavity array for rapid and efficient detection of circulating tumor cells, *Anal. Chem.*, 2010, **82**, 6629–6635.
70 J. S. Kuo, Y. X. Zhao, P. G. Schiro, L. Y. Ng, D. S. W. Lim, J. P. Shelby and D. T. Chiu, Deformability considerations in filtration of biological cells, *Lab Chip*, 2010, **10**, 837–842.
71 L. Li, W. Liu, J. Wang, Q. Tu and R. Liu, Lectin-aided separation of circulating tumor cells and assay of their response to an anticancer drug in an integrated microfluidic device, *Electrophoresis*, 2010, **31**, 3159–3166.
72 H. K. Lin, S. Y. Zheng, A. J. Williams, M. Balic, S. Groshen, H. I. Scher, M. Fleisher, W. Stadler, R. H. Datar, Y. C. Tai and

R. J. Cote, Portable filter-based microdevice for detection and characterization of circulating tumor cells, *Clin. Cancer Res.*, 2010, **16**, 5011–5018.
73 S. J. Tan, R. L. Lakshmi, P. F. Chen, W. T. Lim, L. Yobas and C. T. Lim, Versatile label free biochip for the detection of circulating tumor cells from peripheral blood in cancer patients, *Biosens. Bioelectron.*, 2010, **26**, 1701–1705.
74 A. A. S. Bhagat, H. W. Hou, L. D. Li, C. T. Lim and J. Y. Han, Pinched flow coupled shear-modulated inertial microfluidics for high-throughput rare blood cell separation, *Lab Chip*, 2011, **11**, 1870–1878.
75 S. C. Hur, A. J. Mach and D. Di Carlo, High-throughput size-based rare cell enrichment using microscale vortices, *Biomicrofluidics*, 2011, **5**, 022206.
76 H. S. Moon, K. Kwon, S. I. Kim, H. Han, J. Sohn, S. Lee and H. I. Jung, Continuous separation of breast cancer cells from blood samples using multi-orifice flow fractionation (MOFF) and dielectrophoresis (DEP), *Lab Chip*, 2011, **11**, 1118–1125.
77 S. Y. Zheng, H. K. Lin, B. Lu, A. Williams, R. Datar, R. J. Cote and Y. C. Tai, 3D microfilter device for viable circulating tumor cell (CTC) enrichment from blood, *Biomed. Microdevices*, 2011, **13**, 203–213.
78 K. W. Kwon, S. S. Choi, S. H. Lee, B. Kim, S. N. Lee, M. C. Park, P. Kim, S. Y. Hwang and K. Y. Suh, Label-free, microfluidic separation and enrichment of human breast cancer cells by adhesion difference, *Lab Chip*, 2007, **7**, 1461–1468.
79 C. Couzon, A. Duperray and C. Verdier, Critical stresses for cancer cell detachment in microchannels, *Eur. Biophys. J.*, 2009, **38**, 1035–1047.
80 B. Lincoln, H. M. Erickson, S. Schinkinger, F. Wottawah, D. Mitchell, S. Ulvick, C. Bilby and J. Guck, Deformability-based flow cytometry, *Cytometry, Part A*, 2004, **59**, 203–209.
81 J. Guck, S. Schinkinger, B. Lincoln, F. Wottawah, S. Ebert, M. Romeyke, D. Lenz, H. M. Erickson, R. Ananthakrishnan, D. Mitchell, J. Kas, S. Ulvick and C. Bilby, Optical deformability as an inherent cell marker for testing malignant transformation and metastatic competence, *Biophys. J.*, 2005, **88**, 3689–3698.
82 Y. C. Kim, S. J. Park and J. K. Park, Biomechanical analysis of cancerous and normal cells based on bulge generation in a microfluidic device, *Analyst*, 2008, **133**, 1432–1439.
83 H. W. Hou, Q. S. Li, G. Y. H. Lee, A. P. Kumar, C. N. Ong and C. T. Lim, Deformability study of breast cancer cells using microfluidics, *Biomed. Microdevices*, 2009, **11**, 557–564.
84 J. Chen, M. Abdelgawad, L. M. Yu, N. Shakiba, W. Y. Chien, Z. Lu, W. R. Geddie, M. A. S. Jewett and Y. Sun, Electrodeformation for single cell mechanical characterization, *J. Micromech. Microeng.*, 2011, **21**, 054012.
85 J. Chen, Y. Zheng, Q. Tan, E. Shojaei-Baghini, Y. L. Zhang, J. Li, P. Prasad, L. You, X. Y. Wu and Y. Sun, Classification of cell types using a microfluidic device for mechanical and electrical measurement on single cells, *Lab Chip*, 2011, **11**, 3174–3181.
86 S. C. Hur, N. K. Henderson-MacLennan, E. R. B. McCabe and D. Di Carlo, Deformability-based cell classification and enrichment using inertial microfluidics, *Lab Chip*, 2011, **11**, 912–920.
87 F. H. Labeed, H. M. Coley, H. Thomas and M. P. Hughes, Assessment of multidrug resistance reversal using dielectrophoresis and flow cytometry, *Biophys. J.*, 2003, **85**, 2028–2034.
88 E. G. Cen, C. Dalton, Y. L. Li, S. Adamia, L. M. Pilarski and K. V. I. S. Kaler, A combined dielectrophoresis, traveling wave dielectrophoresis and electrorotation microchip for the manipulation and characterization of human malignant cells, *J. Microbiol. Methods*, 2004, **58**, 387–401.
89 L. M. Broche, F. H. Labeed and M. P. Hughes, Extraction of dielectric properties of multiple populations from dielectrophoretic collection spectrum data, *Phys. Med. Biol.*, 2005, **50**, 2267–2274.
90 S. Chin, M. P. Hughes, H. M. Coley and F. H. Labeed, Rapid assessment of early biophysical changes in K562 cells during apoptosis determined using dielectrophoresis, *Int. J. Nanomed.*, 2006, **1**, 333–337.
91 F. H. Labeed, H. M. Coley and M. P. Hughes, Differences in the biophysical properties of membrane and cytoplasm of apoptotic cells revealed using dielectrophoresis, *Biochim. Biophys. Acta, Gen. Subj.*, 2006, **1760**, 922–929.
92 L. M. Broche, N. Bhadal, M. P. Lewis, S. Porter, M. P. Hughes and F. H. Labeed, Early detection of oral cancer—is dielectrophoresis the answer?, *Oral Oncol.*, 2007, **43**, 199–203.
93 H. M. Coley, F. H. Labeed, H. Thomas and M. P. Hughes, Biophysical characterization of MDR breast cancer cell lines reveals the cytoplasm is critical in determining drug sensitivity, *Biochim. Biophys. Acta, Gen.Subj.*, 2007, **1770**, 601–608.
94 L. Duncan, H. Shelmerdine, M. P. Hughes, H. M. Coley, Y. Hubner and F. H. Labeed, Dielectrophoretic analysis of changes in cytoplasmic ion levels due to ion channel blocker action reveals underlying differences between drug-sensitive and multidrug-resistant leukaemic cells, *Phys. Med. Biol.*, 2008, **53**, N1–N7.
95 S. Shim, P. Gascoyne, J. Noshari and K. Stemke Hale, Dynamic physical properties of dissociated tumor cells revealed by dielectrophoretic field-flow fractionation, *Integr. Biol.*, 2011, **3**, 850–862.
96 F. F. Becker, X. B. Wang, Y. Huang, R. Pethig, J. Vykoukal and P. R. C. Gascoyne, The removal of human leukemia-cells from blood using interdigitated microelectrodes, *J. Phys. D: Appl. Phys.*, 1994, **27**, 2659–2662.
97 F. F. Becker, X. B. Wang, Y. Huang, R. Pethig, J. Vykoukal and P. R. C. Gascoyne, Separation of human breast-cancer cells from blood by differential dielectric affinity, *Proc. Natl. Acad. Sci. U. S. A.*, 1995, **92**, 860–864.
98 P. R. C. Gascoyne, X. B. Wang, Y. Huang and F. F. Becker, Dielectrophoretic separation of cancer cells from blood, *IEEE Trans. Ind. Appl.*, 1997, **33**, 670–678.
99 Y. Huang, X. B. Wang, F. F. Becker and P. R. C. Gascoyne, Introducing dielectrophoresis as a new force field for field-flow fractionation, *Biophys. J.*, 1997, **73**, 1118–1129.
100 J. Cheng, E. L. Sheldon, L. Wu, M. J. Heller and J. P. O'Connell, Isolation of cultured cervical carcinoma cells mixed with peripheral blood cells on a bioelectronic chip, *Anal. Chem.*, 1998, **70**, 2321–2326.
101 Y. Huang, J. Yang, X. B. Wang, F. F. Becker and P. R. C. Gascoyne, The removal of human breast cancer cells from hematopoietic CD34(+) stem cells by dielectrophoretic field-flow-fractionation, *J. Hematother. Stem Cell Res.*, 1999, **8**, 481–490.
102 J. Yang, Y. Huang, X. B. Wang, F. F. Becker and P. R. C. Gascoyne, Cell separation on microfabricated electrodes using dielectrophoretic/gravitational field flow fractionation, *Anal. Chem.*, 1999, **71**, 911–918.
103 X. B. Wang, J. Yang, Y. Huang, J. Vykoukal, F. F. Becker and P. R. C. Gascoyne, Cell separation by dielectrophoretic field-flow-fractionation, *Anal. Chem.*, 2000, **72**, 832–839.
104 Y. Huang, S. Joo, M. Duhon, M. Heller, B. Wallace and X. Xu, Dielectrophoretic cell separation and gene expression profiling on microelectronic chip arrays, *Anal. Chem.*, 2002, **74**, 3362–3371.
105 L. Altomare, M. Borgatti, G. Medoro, N. Manaresi, M. Tartagni, R. Guerrieri and R. Gambari, Levitation and movement of human tumor cells using a printed circuit board device based on software-controlled dielectrophoresis, *Biotechnol. Bioeng.*, 2003, **82**, 474–479.
106 C. M. Das, F. Becker, S. Vernon, J. Noshari, C. Joyce and P. R. C. Gascoyne, Dielectrophoretic segregation of different human cell types on microscope slides, *Anal. Chem.*, 2005, **77**, 2708–2719.
107 X. Y. Hu, P. H. Bessette, J. R. Qian, C. D. Meinhart, P. S. Daugherty and H. T. Soh, Marker-specific sorting of rare cells using dielectrophoresis, *Proc. Natl. Acad. Sci. U. S. A.*, 2005, **102**, 15757–15761.
108 J. Park, B. Kim, S. K. Choi, S. Hong, S. H. Lee and K. I. Lee, An efficient cell separation system using 3D-asymmetric microelectrodes, *Lab Chip*, 2005, **5**, 1264–1270.
109 U. Kim, C. W. Shu, K. Y. Dane, P. S. Daugherty, J. Y. J. Wang and H. T. Soh, Selection of mammalian cells based on their cell-cycle phase using dielectrophoresis, *Proc. Natl. Acad. Sci. U. S. A.*, 2007, **104**, 20708–20712.
110 M. Cristofanilli, S. Krishnamurthy, C. M. Das, J. M. Reuben, W. Spohn, J. Noshari, F. Becker and P. R. Gascoyne, Dielectric cell separation of fine needle aspirates from tumor xenografts, *J. Sep. Sci.*, 2008, **31**, 3732–3739.
111 Y. J. Kang, D. Q. Li, S. A. Kalams and J. E. Eid, DC-dielectrophoretic separation of biological cells by size, *Biomed. Microdevices*, 2008, **10**, 243–249.
112 J. An, J. Lee, S. H. Lee, J. Park and B. Kim, Separation of malignant human breast cancer epithelial cells from healthy epithelial cells using an advanced dielectrophoresis-activated cell sorter (DACS), *Anal. Bioanal. Chem.*, 2009, **394**, 801–809.



 

113 P. R. C. Gascoyne, J. Noshari, T. J. Anderson and F. F. Becker, Isolation of rare cells from cell mixtures by dielectrophoresis, *Electrophoresis*, 2009, **30**, 1388–1398.
114 S. Kostner, S. van den Driesche, W. Witarski, S. Pastorekova and M. J. Vellekoop, Guided dielectrophoresis: a robust method for continuous particle and cell separation, *IEEE Sens. J.*, 2010, **10**, 1440–1446.
115 A. C. Sabuncu, J. A. Liu, S. J. Beebe and A. Beskok, Dielectrophoretic separation of mouse melanoma clones, *Biomicrofluidics*, 2010, **4**, 021101.
116 F. Yang, X. M. Yang, H. Jiang, P. Bulkhaults, P. Wood, W. Hrushesky and G. R. Wang, Dielectrophoretic separation of colorectal cancer cells, *Biomicrofluidics*, 2010, **4**, 013204.
117 A. Alazzam, I. Stiharu, R. Bhat and A. N. Meguerditchian, Interdigitated comb-like electrodes for continuous separation of malignant cells from blood using dielectrophoresis, *Electrophoresis*, 2011, **32**, 1327–1336.
118 K. H. Han, A. Han and A. B. Frazier, Microsystems for isolation and electrophysiological analysis of breast cancer cells from blood, *Biosens. Bioelectron.*, 2006, **21**, 1907–1914.
119 Y. Cho, H. S. Kim, A. B. Frazier, Z. G. Chen, D. M. Shin and A. Han, Whole-cell impedance analysis for highly and poorly metastatic cancer cells, *J. Microelectromech. Syst.*, 2009, **18**, 808–817.
120 J. Mamouni and L. Yang, Interdigitated microelectrode-based microchip for electrical impedance spectroscopic study of oral cancer cells, *Biomed. Microdevices*, 2011, **13**, 1075–1088.
121 L. J. Yang, L. R. Arias, T. S. Lane, M. D. Yancey and J. Mamouni, Real-time electrical impedance-based measurement to distinguish oral cancer cells and non-cancer oral epithelial cells, *Anal. Bioanal. Chem.*, 2011, **399**, 1823–1833.
122 Y. H. Xu, X. R. Yang and E. K. Wang, Review: aptamers in microfluidic chips, *Anal. Chim. Acta*, 2010, **683**, 12–20.
123 J. Voldman, Electrical forces for microscale cell manipulation, *Annu. Rev. Biomed. Eng.*, 2006, **8**, 425–454.
124 F. E. H. Tay, L. M. Yu and C. Iliescu, Particle manipulation by miniaturised dielectrophoretic devices, *Def. Sci. J.*, 2009, **59**, 595–604.
125 C. Zhang, K. Khoshmanesh, A. Mitchell and K. Kalantar-zadeh, Dielectrophoresis for manipulation of micro/nano particles in microfluidic systems, *Anal. Bioanal. Chem.*, 2010, **396**, 401–420.
126 K. Khoshmanesh, S. Nahavandi, S. Baratchi, A. Mitchell and K. Kalantar-zadeh, Dielectrophoretic platforms for bio-microfluidic systems, *Biosens. Bioelectron.*, 2011, **26**, 1800–1814.
127 D. H. Kim, P. K. Wong, J. Park, A. Levchenko and Y. Sun, Microengineered platforms for cell mechanobiology, *Annu. Rev. Biomed. Eng.*, 2009, **11**, 203–233.
128 O. Loh, A. Vaziri and H. Espinosa, The potential of MEMS for advancing experiments and modeling in cell mechanics, *Exp. Mech.*, 2009, **49**, 105–124.
129 S. A. Vanapalli, M. H. G. Duits and F. Mugele, Microfluidics as a functional tool for cell mechanics, *Biomicrofluidics*, 2009, **3**, 012006.
130 J. Rajagopalan and M. T. A. Saif, MEMS sensors and microsystems for cell mechanobiology, *J. Micromech. Microeng.*, 2011, **21**, 054002.
131 X. Y. R. Zheng and X. Zhang, Microsystems for cellular force measurement: a review, *J. Micromech. Microeng.*, 2011, **21**, 054003.
132 Y. Zheng and Y. Sun, Microfluidic devices for mechanical characterisation of single cells in suspension, *Micro Nano Lett.*, 2011, **6**, 327–331.
133 H. Morgan, T. Sun, D. Holmes, S. Gawad and N. G. Green, Single cell dielectric spectroscopy, *J. Phys. D: Appl. Phys.*, 2007, **40**, 61–70.
134 A. Valero, T. Braschler and P. Renaud, A unified approach to dielectric single cell analysis: impedance and dielectrophoretic force spectroscopy, *Lab Chip*, 2010, **10**, 2216–2225.
135 K. C. Cheung, M. Di Berardino, G. Schade-Kampmann, M. Hebeisen, A. Pierzchalski, J. Bocsi, A. Mittag and A. Tarnok, Microfluidic impedance-based flow cytometry, *Cytometry, Part A*, 2010, **77**, 648–666.
136 T. Sun and H. Morgan, Single-cell microfluidic impedance cytometry: a review, *Microfluid. Nanofluid.*, 2010, **8**, 423–443.
137 K. Hoshino, Y.-Y. Huang, N. Lane, M. Huebschman, J. W. Uhr, E. P. Frenkel and X. Zhang, Microchip-based immunomagnetic detection of circulating tumor cells, *Lab Chip*, 2011, **11**, 3449–3457.
138 M. Cristofanilli, G. De Gasperis, L. S. Zhang, M. C. Hung, P. R. C. Gascoyne and G. N. Hortobagyi, Automated electrorotation to reveal dielectric variations related to HER-2/neu overexpression in MCF-7 sublines, *Clin. Cancer Res.*, 2002, **8**, 615–619.